



Scholars Research Library

Der Pharma Chemica, 2015, 7(10):77-88
(<http://derpharmachemica.com/archive.html>)



ISSN 0975-413X
CODEN (USA): PCHHAX

Correlated DFT and electrochemical study on inhibition behavior of ethyl 6-amino-5-cyano-2-methyl-4-(p-tolyl)-4H-pyran-3-carboxylate for the corrosion of mild steel in HCl

M. El Hezzat¹, M. Assouag², H. Zarrok³, Z. Benzekri⁴, A. El Assyry⁵, S. Boukhris⁴, A. Souizi⁴, M. Galai⁶, R. Tourir^{6,7}, M. Ebn Touhami⁶, H. Oudda³ and A. Zarrouk⁸

¹Laboratoire de Physico-Chimie des Matériaux Vitreux et Cristallisés, Faculté des Sciences, Université Ibn Tofail, Kenitra, Morocco

²Equipe Matériaux Avancés et Applications ENSAM, Université Moulay Ismail, Al Mansour, Meknès, Morocco

³Laboratoire des procédés de séparation, Faculté des Sciences, Université Ibn Tofail, Kenitra, Morocco

⁴Laboratoire de Chimie Organique, Organométallique et Théorique, Faculté des Sciences, Université Ibn Tofail, Kenitra, Morocco

⁵Laboratoire d'Optoélectronique et de Physico-chimie des Matériaux (Unité associée au CNRST), Département de Physique, Université Ibn Tofail, Kenitra, Maroc

⁶Ingénierie des Matériaux et d'Environnement: Modélisation et application, Faculté des Sciences, Université Ibn Tofail, Kenitra, Morocco

⁷Centre Régional des métiers de l'éducation et de la formation (CRMEF), Avenue Allal Al Fassi, Madinat Al Irfane, Rabat, Morocco

⁸LCAE-URAC18, Faculty of Science, Mohammed first University, Oujda, Morocco

ABSTRACT

The inhibition effect of ethyl 6-amino-5-cyano-2-methyl-4-(p-tolyl)-4H-pyran-3-carboxylate (Pyr2) on the corrosion of mild steel in 1.0 M HCl was investigated by electrochemical (potentiodynamic polarization and electrochemical impedance spectroscopic studies) and theoretical methods. The potentiodynamic polarization was carried at different temperatures ranging from 298 to 328 K. In all the studies, Inhibition efficiency increases with increase in concentrations of Pyr2 but decreases with rise in the temperature. Potentiodynamic polarization measurements confirmed that the inhibitive action of this compound is of mixed type. The activation parameters and thermodynamic values responsible for the adsorption were discussed. The adsorption of the inhibitor on mild steel surface has been found to obey the Langmuir isotherm. Density functional theory (DFT) at the B3LYP/6-311G(d,p) basis set level was performed. Excellent correlation was found between experimental and theoretical results.

Keywords: Mild steel, HCl, Corrosion inhibition, Pyrane derivative, Electrochemical techniques, DFT

INTRODUCTION

Excessive corrosion attacks occur on mild steel surfaces deployed in service in aqueous aggressive environments. The dissolution of metals in such environment can be significantly suppressed by the addition of few compounds to the environment that adsorb on metal decrease its dissolution. Several organic molecules containing N, O, and S were reported as corrosion retarding agents for mild steel in acid solutions [1-18]. The nature of the adsorption of inhibitor depends on the type of metal, structure of the molecule, and the strength of the electrolyte.

The corrosion of mild steel may proceed through various mechanisms and manifest in different forms in any given environment. Accordingly, in order to be considered effective, an inhibitor may require performing through various

functions. The adsorption of inhibitors is by the attractive forces arose between the inhibitor molecules and the metal surface. The electrostatic force in-between the charged metal surface and inhibitors is physisorption. The process of forming coordinate bond between the unshared electrons of the inhibitors and the metal surface is known as chemisorption. The adsorption will be favored by the presence of heteroatoms (S, N, and O) and their lone-pair of electrons and aromatic rings in the inhibitors [19-34].

The aim of the present work is to investigate the effects of ethyl 6-amino-5-cyano-2-methyl-4-(p-tolyl)-4H-pyran-3-carboxylate (Pyr2) as corrosion inhibitor for mild steel in 1.0 M HCl solution using electrochemical techniques. Thermodynamic activation parameters were evaluated from experimental data. The relationships between the inhibition performances of the investigated inhibitor in 1.0 M HCl and some quantum chemical parameters, such as the highest occupied molecular orbital energy (E_{HOMO}), the lowest unoccupied molecular orbital energy (E_{LUMO}), the energy gap between E_{LUMO} and E_{HOMO} ($\Delta E_{\text{LUMO-HOMO}}$), dipole moments, electronegativity (χ), global chemical hardness (η) and the fraction of electrons transferred from the inhibitor to the iron surface (ΔN). The molecular structure of Pyr2 is given in Figure 1.

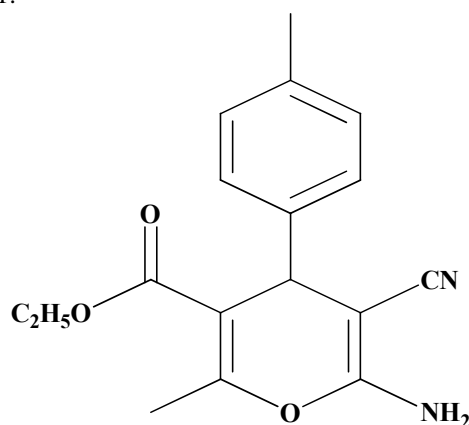


Figure 1: Molecular structure of Pyr2

MATERIALS AND METHODS

Materials

The steel used in this study is a mild steel with a chemical composition (in wt%) of 0.09%P, 0.01 % Al, 0.24 % Si, 0.47 % Mn, 0.11 % C, 0.12 % Cr, 0.02 % Mo, 0.1 % Ni, 0.03 % Al, 0.14 % Cu, 0.06 % W, <0.0012 % Co, <0.003 % V and the remainder iron (Fe). The steel samples were pre-treated prior to the experiments by grinding with SiC abrasive paper of grade respectively 220, 400, 800, 1000 and 1200; rinsed with distilled water, degreased in acetone, washed again with bidistilled water and then dried at room temperature before use.

Solutions

The aggressive solutions of 1.0 M HCl were prepared by dilution of analytical grade 37% HCl with distilled water. The concentration range of ethyl 6-amino-5-cyano-2-methyl-4-(p-tolyl)-4H-pyran-3-carboxylate (Pyr2) used was 10^{-6} M to 10^{-3} M.

Electrochemical measurements

The electrochemical measurements were carried out using Volta lab (Tacussel- Radiometer PGZ 100) potentiostat and controlled by Tacussel corrosion analysis software model (Voltmaster 4) at under static condition. The corrosion cell used had three electrodes. The reference electrode was a saturated calomel electrode (SCE). A platinum electrode was used as auxiliary electrode of surface area of 1 cm^2 . The working electrode was mild steel of the surface 1.0 cm^2 . All potentials given in this study were referred to this reference electrode. The working electrode was immersed in test solution for 30 min to a establish steady state open circuit potential (E_{ocp}). After measuring the E_{ocp} , the electrochemical measurements were performed. All electrochemical tests have been performed in aerated solutions at 298 K. The EIS experiments were conducted in the frequency range with high limit of 100 kHz and different low limit 0.1 Hz at open circuit potential, with 10 points per decade, at the rest potential, after 30 min of acid immersion, by applying 10 mV ac voltage peak-to-peak. Nyquist plots were made from these experiments. The best semicircle can be fit through the data points in the Nyquist plot using a non-linear least square fit so as to give the intersections with the x -axis.

The inhibition efficiency of the inhibitor was calculated from the charge transfer resistance values using the following equation:

$$\eta_z \% = \frac{R_{ct}^i - R_{ct}^{\circ}}{R_{ct}^i} \times 100 \quad (1)$$

Where, R_{ct}° and R_{ct}^i are the charge transfer resistance in absence and in presence of inhibitor, respectively.

After ac impedance test, the potentiodynamic polarization measurements of mild steel substrate in inhibited and uninhibited solution were scanned from cathodic to the anodic direction, with a scan rate of 0.5 mV s^{-1} . The potentiodynamic data were analysed using the polarization VoltaMaster 4 software. The linear Tafel segments of anodic and cathodic curves were extrapolated to corrosion potential to obtain corrosion current densities (I_{corr}). The inhibition efficiency was evaluated from the measured I_{corr} values using the following relationship:

$$\eta_{\text{Tafel}}(\%) = \frac{I_{\text{corr}} - I_{\text{corr}(i)}}{I_{\text{corr}}} \times 100 \quad (2)$$

where I_{corr} and $I_{\text{corr}(i)}$ are the corrosion current densities for steel electrode in the uninhibited and inhibited solutions, respectively.

Quantum chemical calculations

Complete geometrical optimizations of the investigated molecules are performed using DFT (density functional theory) with the Beck's three parameter exchange functional along with the Lee-Yang-Parr nonlocal correlation functional (B3LYP) [35-37] with 6-31G* basis set is implemented in Gaussian 03 program package [38]. This approach is shown to yield favorable geometries for a wide variety of systems. This basis set gives good geometry optimizations. The geometry structure was optimized under no constraint. The following quantum chemical parameters were calculated from the obtained optimized structure: The highest occupied molecular orbital (E_{HOMO}) and the lowest unoccupied molecular orbital (E_{LUMO}), the energy difference (ΔE) between E_{HOMO} and E_{LUMO} , dipole moment (μ), electron affinity (A), ionization potential (I) and the fraction of electrons transferred (ΔN).

RESULTS AND DISCUSSION

EIS measurements

The EIS analysis was done on mild steel in 1.0 M HCl in the absence and presence of different concentrations of the Pyr2 in order to describe the kinetics and characteristics of the electrochemical reactions occurring on the metal/electrolyte interface. Fig. 2(a) represents the Nyquist plots for mild steel in the absence and presence of the studied Pyr2 which show the imperfect semicircles resulted due to surface roughness and inhomogeneities. The accumulation of corrosion products and formation of pits and cracks result into the production of surface roughens and inhomogeneities. The impedance nature of mild steel dissolution can be explained by involvement of an equivalent circuit (Fig. 2b) consisting of the solution resistance (R_s), the charge transfer resistance (R_{ct}) and double layer capacitance (C_{dl}) as described elsewhere [39]. The double layer capacitance was derived using following relation:

$$C_{dl} = \frac{Y_0 \omega^{n-1}}{\sin(n(\pi/2))} \quad (3)$$

where Y_0 is the amplitude comparable to a capacitance (with a $\mu\text{F cm}^{-2}$), ω is the angular frequency, and n is the phase shift, which is a measure of surface roughness. Generally, the high value of n associated with low surface roughness and high surface coverage. To find more accurate fit, the constant phase element (CPE) was used in our present study rather than double layer capacitance. The impedance of the CPE (Z_{CPE}) can be represented as follows:

$$Z_{\text{CPE}} = \left(\frac{1}{Y_0} \right) [(j\omega)_n]^{-1} \quad (4)$$

where, j is the imaginary unit. The behavior of the CPE can be explained on the basis of values on the n . Generally, if the value of n equals to +1, 0, and -1, the CPE behaves as resistance, capacitance and inductance, respectively [40].

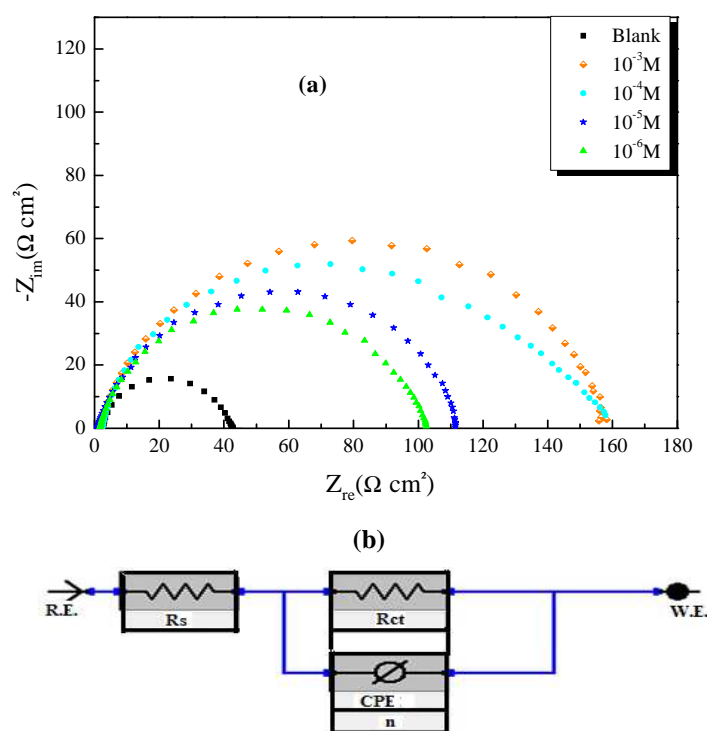


Figure 2: (a): Nyquist plot for mild steel in 1.0 M HCl without and with various concentrations of Pyr2; (b): equivalent circuit model used to fit the EIS data

The calculated values of n in absence and presence Pyr2 at different concentrations are given in Table 1. Several impedance parameters such as R_s , R_{ct} , C_{dl} , n and $\eta_z\%$ were derived using above equivalent circuit shown in Fig. 2(b) and are given in Table 1. From the results shown in Table 1 it was observed that values of R_{ct} increase whereas the values of C_{dl} decrease in the presence of studied compound. This increase in R_{ct} and decrease in C_{dl} values in the presence of Pyr2 are attributed due to a decrease in local dielectric constant and/or to an increase in the thickness of the electrical double layer [41,42]. These results suggest that the studied Pyr2 inhibit mild steel corrosion by adsorbing at the metal/electrolyte interfaces.

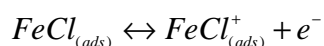
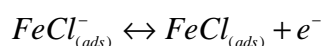
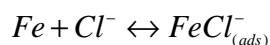
Table 1: Corrosion parameters obtained by impedance measurements for mild steel in 1.0 M HCl at various concentrations of Pyr2

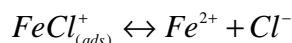
| Medium | Conc (M) | R_s ($\Omega \text{ cm}^2$) | R_{ct} ($\Omega \text{ cm}^2$) | n | C_{dl} ($\mu\text{F}/\text{cm}^2$) | η_z (%) |
|--------|-----------|---------------------------------|------------------------------------|------|--|--------------|
| Blank | 1.0 | 2.5 | 40 | 0.80 | 211 | — |
| Pyr2 | 10^{-3} | 1.2 | 160 | 0.85 | 142 | 75.0 |
| | 10^{-4} | 1.0 | 157 | 0.84 | 153 | 74.5 |
| | 10^{-5} | 0.5 | 111 | 0.84 | 170 | 64.0 |
| | 10^{-6} | 0.8 | 102 | 0.83 | 203 | 61.0 |

Potentiodynamic polarization measurements

Effect of concentration inhibitor

Potentiodynamic polarization curves of mild steel in 1.0 M HCl in the absence and presence of 10^{-6} to 10^{-3} M concentrations of Pyr2 is given in Figure 3. The potentiodynamic polarization parameters i.e. Corrosion potential (E_{corr}), cathodic Tafel slopes (β_c), corrosion current density (I_{corr}) and percentage inhibition efficiency ($\eta_{Tafel}\%$) were also calculated and given in Table 2. Complete dissolution of mild steel in acid solution can be divided into two half reactions, one is the cathodic half reaction another is the anodic half reaction. The anodic half reaction involves dissolution mild steel through oxidation process as described earlier [43-45]:





whereas, cathodic reaction involves the hydrogen evolution through reduction process according to following steps [43-45]:

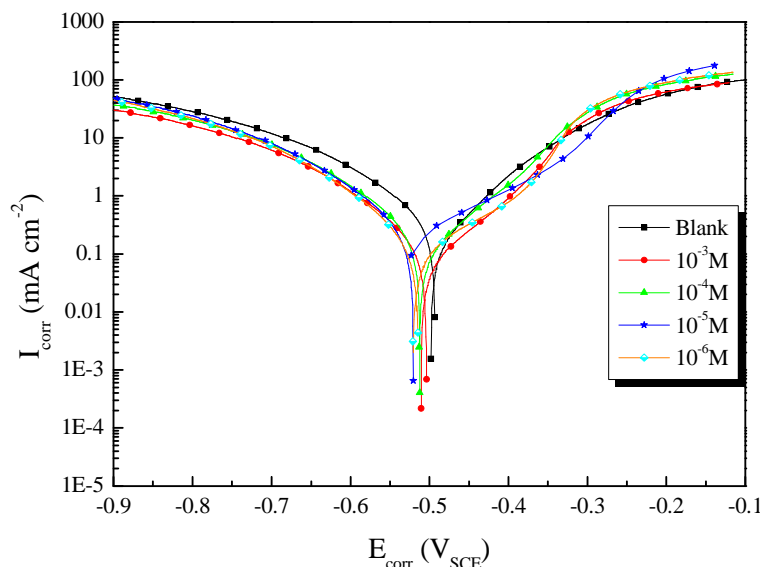
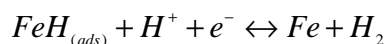
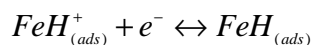
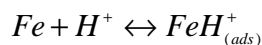


Figure 3: Potentiodynamic polarization curves for the corrosion of mild steel in 1.0 M HCl solution without and with various concentrations of Pyr2 at 298 K

The potentiodynamic curves show that there is a clear reduction of both the anodic and cathodic currents in the presence of Pyr2 compared with those for the blank solution. It is clear that the cathodic reaction (hydrogen evolution) and the anodic reaction (dissolution metal) were inhibited. From table 2 we can observed that both anodic Tafel slope (β_a) and cathodic Tafel slope (β_c) values do not change much in the presence of Pyr2 with respect to blank [46]. There is no definite trend observed in the E_{corr} values in the presence of Pyr2. In literature [47], it has been reported that (i) if the displacement in E_{corr} is > 85 mV with respect to E_{corr} , the inhibitor can be seen as a cathodic or anodic type and (ii) if displacement in E_{corr} is < 85 , the inhibitor can be seen as mixed type. In the present study, shift in E_{corr} values is in the range of 4-21 mV, suggesting that Pyr2 acted as mixed type of inhibitor [48,49].

Table 2: Effect of concentration of Pyr2 on the electrochemical parameters calculated using potentiodynamic polarization technique for the corrosion of mild steel in 1.0 M HCl at 298 K

| Medium | Conc (M) | $-E_{corr}$ (mV/SCE) | $-\beta_c$ (mV/dec) | β_a (mV/dec) | I_{corr} ($\mu A/cm^2$) | η_{Tafel} (%) |
|--------|-----------|----------------------|---------------------|--------------------|-----------------------------|--------------------|
| Blank | 1.0 | 498 | 105 | 99 | 467 | — |
| Pyr2 | 10^{-3} | 502 | 88 | 87 | 109 | 76.6 |
| | 10^{-4} | 511 | 92 | 83 | 122 | 74.0 |
| | 10^{-5} | 519 | 88 | 82 | 169 | 64.0 |
| | 10^{-6} | 507 | 90 | 99 | 180 | 61.5 |

Effect of temperature

The change of the corrosion rate with the temperature was studied in the absence and in the presence of Pyr2 in 1.0 M HCl. For this purpose, potentiodynamic polarization measurements were performed at different temperatures from 298 to 328 K in the absence and in the presence of different concentrations of Pyr2 (Figures 4 and 5). Figures 4 and 5 show that raising the temperature has no significant effect on the corrosion potentials but leads to a higher corrosion current density (I_{corr}). With increasing temperature, the steel corrosion resistance decreased in both the presence and absence of inhibitor.

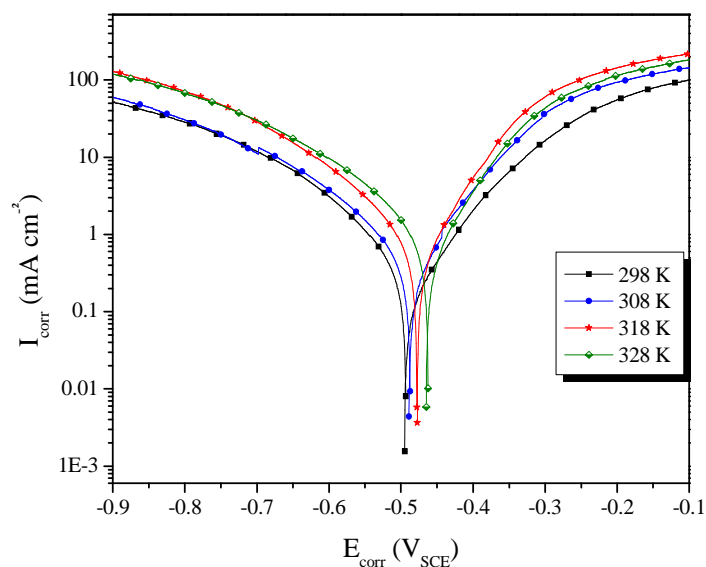


Figure 4: Anodic and cathodic polarization curves for steel in 1.0 M HCl without inhibitor at different temperatures

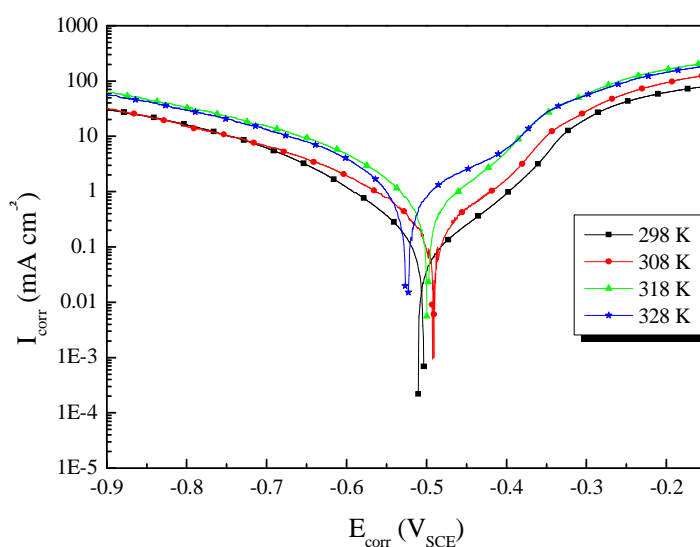


Figure 5: Anodic and cathodic polarization curves for steel in 1.0 M HCl with 10^{-3} M of Pyr2 at different temperatures

Table 3: Various corrosion parameters for mild steel in 1.0 M HCl in absence and presence of optimum concentration of Pyr2 at different temperatures

| Medium | Temp (K) | $-E_{\text{corr}}$ (mV _{SCE}) | I_{corr} ($\mu\text{A cm}^{-2}$) | $-\beta_c$ (mV/dec) | η_{Tafel} (%) |
|--------|----------|---|---|---------------------|---------------------------|
| Blank | 298 | 498 | 467 | 170 | — |
| | 308 | 491 | 800 | 178 | — |
| | 318 | 475 | 1432 | 165 | — |
| | 328 | 465 | 2052 | 151 | — |
| Pyr2 | 298 | 502 | 109 | 88 | 76.6 |
| | 308 | 489 | 287 | 96 | 64.0 |
| | 318 | 498 | 580 | 93 | 59.0 |
| | 328 | 524 | 901 | 105 | 56.0 |

The electrochemical parameters were extracted and summarized in Table 3. The dependence of the corrosion rate on temperature can be expressed by the Arrhenius equation [50]:

$$I_{corr} = k \exp\left(-\frac{E_a}{RT}\right) \quad (5)$$

where E_a is the apparent activation corrosion energy, R is the universal gas constant and k is the Arrhenius pre-exponential constant. Arrhenius plots for the corrosion density of mild steel in the case of Pyr2 are given in Fig.7. Values of apparent activation energy of corrosion (E_a) for mild steel in 1.0 M HCl with the absence and presence of Pyr2 were determined from the slope of $\ln(I_{corr})$ versus $1/T$ plots and shown in Table 4.

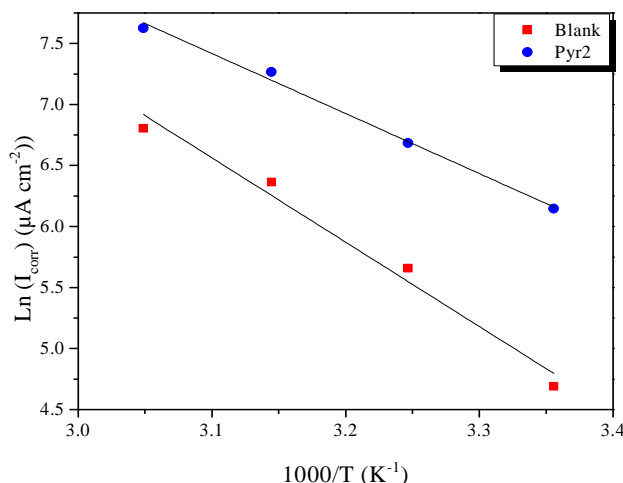


Figure 7: Arrhenius plots of mild steel in 1.0 M HCl with and without 10^{-3} M of Pyr2

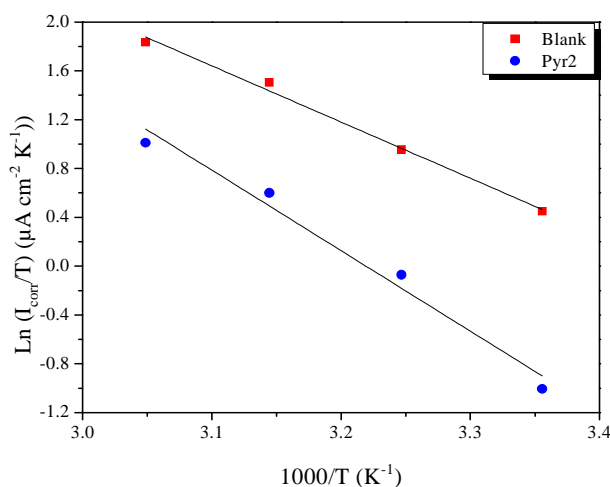


Figure 8: Transition Arrhenius plots of mild steel in 1.0 M HCl with and without 10^{-3} M of Pyr2

Table 4: The values of activation parameters E_a , ΔH_a and ΔS_a for mild steel in 1.0 M HCl in the absence and presence of 10^{-3} M of Pyr2

| Medium | E_a (kJ/mol) | ΔH_a (kJ/mol) | ΔS_a (J/mol K) |
|--------|-------------------|--------------------------|---------------------------|
| Blank | 40.88 | 38.29 | -65.21 |
| Pyr2 | 57.45 | 54.85 | -20.96 |

According to the report in literature [51], higher value of E_a was considered as physisorption that occurred in the first stage. Because the electrochemical corrosion is relevant to heterogeneous reactions, the preexponential factor k in the Arrhenius equation is related to the number of active centers. There are two possibilities about these active centers with different E_a on the metal surface: (1) the activation energy in the presence of inhibitors is lower than that of pure acidic medium, namely $E_a(-inh) < E_a(HCl)$, which suggests a smaller number of more active sites remain uncovered in the corrosion process; (2) the activation energy in the presence of inhibitor is higher than that of pure

acidic medium, $E_a(\text{inh}) > E_a(\text{HCl})$, which represents the inhibitor adsorbed on most active adsorption sites (having the lowest energy) and the corrosion takes place chiefly on the active sites (having higher energy).

The data in Table 4 specifically indicate that the value of E_a in the presence of Pyr2 is larger than that in the absence of Pyr2. Thus, it is clear that the adsorption of Pyr2 on mild steel surface blocks the active sites from acid solution and consequently increases the apparent activation energy. Then, it can be suggested that the Pyr2 adsorb by physisorption on metallic surface.

Activation parameters like enthalpy (ΔH_a) and entropy (ΔS_a) for the dissolution of mild steel in 1.0 M HCl in the absence and presence of 10^{-3} M Pyr2 were calculated from the transition state equation (Eq. (6)) [52]:

$$I_{\text{corr}} = \frac{RT}{Nh} \exp\left(\frac{\Delta S_a}{R}\right) \exp\left(-\frac{\Delta H_a}{RT}\right) \quad (6)$$

where I_{corr} is the corrosion rate, A is the pre-exponential factor, h is Planck's constant, N is the Avogadro number, R is the universal gas constant, ΔH_a is the enthalpy of activation and ΔS_a is the entropy of activation.

Fig. 8 showed the Arrhenius plots of $\ln(I_{\text{corr}}/T)$ versus $1/T$ gave straight lines with slope ($-\Delta H_a/R$) and intercept ($\ln R/Nh + \Delta S_a/R$) from which ΔH_a and ΔS_a values were calculated. The activation parameters are given in Table 4.

The positive sign of the enthalpies ΔH_a reflects the endothermic nature of the steel dissolution process whereas large negative values of entropies ΔS_a from Pyr2 imply that the activated complex in the rate determining step represents an association rather than a dissociation step, meaning that a decrease in disordering takes place on going from reactants to the activated complex [53,54].

Adsorption Isotherm

The adsorption on the corroding surfaces never reaches the real equilibrium and tends to reach an adsorption steady state. However, when the corrosion rate is sufficiently small, the adsorption steady state has a tendency to become a quasi-equilibrium state. In this case, it is reasonable to consider the quasi-equilibrium adsorption in a thermodynamic way using the appropriate equilibrium isotherms. The efficiency of the Pyr2 as a successful corrosion inhibitor mainly depends on its adsorption ability on the metal surface. So, it is essential to know the mode of adsorption and the adsorption isotherm that can give valuable information on the interaction of inhibitor and metal surface.

The surface coverage values, θ ($\theta = (\eta_{\text{Tafel}}/\%) / 100$), for different concentrations of Pyr2 were used to explain the best adsorption isotherm. A plot of C_{inh}/θ versus C_{inh} (Figure 9) gives a straight line with an average correlation coefficient of 0.99999 and a slope of nearly unity suggests that the adsorption of Pyr2 molecules obeys Langmuir adsorption isotherm, which can be expressed by the following equation:

$$\frac{C_{\text{inh}}}{\theta} = \frac{1}{K_{\text{ads}}} + C_{\text{inh}} \quad (7)$$

where C_{inh} is the inhibitor concentration and K_{ads} is the equilibrium constant for adsorption-desorption process. From the intercepts of the straight lines on the C_{inh}/θ -axis (Figure 9), K_{ads} can be calculated which is related to free energy of adsorption, $\Delta G_{\text{ads}}^\circ$ as given by

$$K_{\text{ads}} = \left(\frac{1}{55.5}\right) \exp\left(-\frac{\Delta G_{\text{ads}}^\circ}{RT}\right) \quad (8)$$

where R is gas constant and T is absolute temperature of experiment and the constant value of 55.5 is the concentration of water in solution in mol dm^{-3} . The thermodynamic parameters are listed in Table 5.

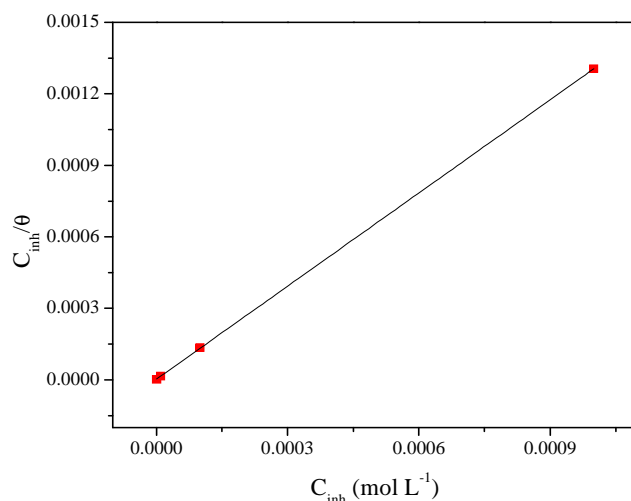


Figure 9: Adsorption isotherm according to Langmuir's model derived from weight loss measurement

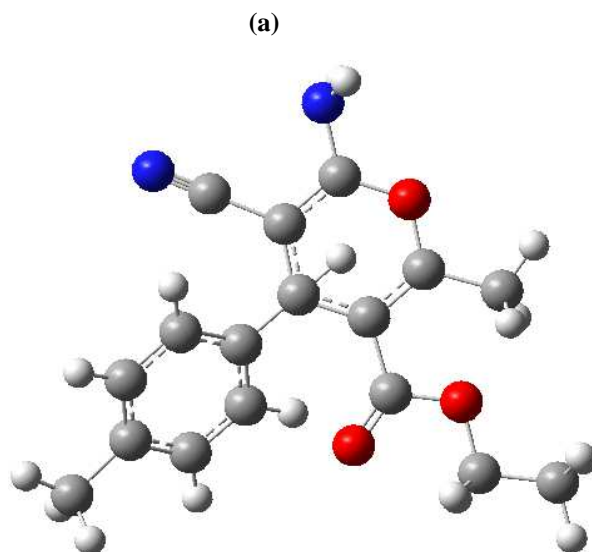
Table 5: Thermodynamic parameters for the adsorption of Pyr2 in 1.0 M HCl on the mild steel at 298K

| K_{ads} (M^{-1}) | R^2 | ΔG_{ads}° (kJ/mol) |
|---------------------------|---------|--------------------------------------|
| 400036.8 | 0.99999 | -41.91 |

From table 5, the negative values of standard free energy of adsorption indicate spontaneous adsorption of organic molecules on metallic surface and also the strong interaction between inhibitor molecules and mild steel surface [55,56]. Generally, the standard free energy values of -20 kJ mol^{-1} or less negative are associated with an electrostatic interaction between charged molecules and charged metal surface (physical adsorption); those of -40 kJ mol^{-1} or more negative involves charge sharing or transfer from the inhibitor molecules to the metal surface to form a co-ordinate covalent bond (chemical adsorption) [57,58]. Based on the literature [59], the calculated ΔG_{ads}° value in this work indicates that the adsorption mechanism of Pyr2 on mild steel is chemisorption.

Quantum chemical study

In order to investigate the correlation between the molecular structure of the inhibitor and its inhibition effect, quantum chemical calculations have been performed. Fig. 10 shows the optimized geometric structure and the electron density distribution of both HOMO and LUMO. The related quantum chemical parameters including E_{HOMO} , E_{LUMO} , ΔE , μ , electron affinity (A), ionization potential (I) and the fraction of electrons transferred (ΔN) are given in Table 6. From Fig. 10, it can be found that the electron density distribution of both HOMO and LUMO are localized on the whole molecule.



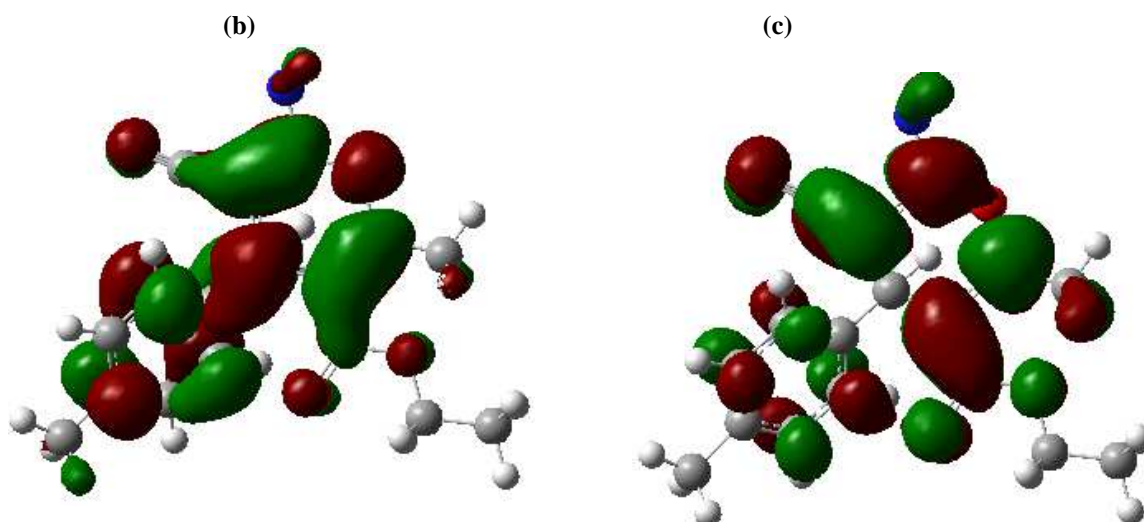


Figure 10: Optimized geometric structure (a) and the electron density distributions of both HOMO (b) and LUMO (c) for the Pyr2

It is well known that HOMO is often associated with the ability of the molecule to donate electron and high E_{HOMO} value means a strong electron-donating ability [60-64], while LUMO indicates the electron-accepting ability of the molecule and the lower value of E_{LUMO} indicates that the molecule would more probably accept electrons [60-64]. The energy gap (ΔE) between HOMO and LUMO reflects the stability of the molecule, a smaller ΔE implies that the molecule is much easier to be polarized and adsorbed on the metal surface [60,63-65]. In addition, owing to the dipole-dipole interaction between molecules and metal surface, high values of the dipole moment can lead to stronger inhibition [63,64]. The results of Table 6 shows that the values of E_{HOMO} and E_{LUMO} are lower, which indicates the Pyr2 cation is more likely to accept electrons rather than donate electrons. The μ of the Pyr2 cation is higher than that of H_2O [63]. The high value of μ probably increases the adsorption between the Pyr2 cation and metal surface [63].

Table 6: The computed molecular parameters for Pyr2 compound

| E_{HOMO} (eV) | E_{LUMO} (eV) | ΔE gap (eV) | μ (debye) | I (eV) | A (eV) | ΔN |
|-----------------|-----------------|---------------------|---------------|----------|----------|------------|
| -6.3130 | -4.9797 | 1.3333 | 7.4032 | 6.3130 | 4.9797 | 1.015263 |

In addition the number of transferred electrons (ΔN) was also calculated depending on the quantum chemical method [66]:

$$\Delta N = \frac{\chi_{Fe} - \chi_{inh}}{2(\eta_{Fe} + \eta_{inh})} \quad (9)$$

where χ_{Fe} and χ_{inh} denote the absolute electronegativity of iron and the inhibitor molecule, respectively; η_{Fe} and η_{inh} denote the absolute hardness of iron and the inhibitor molecule, respectively. These quantities are related to electron affinity (A) and ionization potential (I) as follows:

$$\chi = \frac{I + A}{2}; \quad \eta = \frac{I - A}{2} \quad (10)$$

I and A are related [67] in turn to E_{HOMO} and E_{LUMO} as follows:

$$I = -E_{HOMO}; \quad A = -E_{LUMO} \quad (11)$$

For iron atom, a theoretical χ value of 7 eV mol⁻¹ and η value of 0 eV mol⁻¹ were used [68] to calculate the number of electrons transferred (ΔN) from inhibitor to the iron atom. The number of transferred electrons depends strongly on what the actual quantum chemical method employed for computation. Furthermore, the expression ‘‘number of transferred electrons’’ is the wording ‘‘electron-donating ability’’, which does not imply that the figures of ΔN actually indicate the number of electrons leaving the donor and entering the acceptor molecule.

Using Eq. 9, the value of electron-donating ability (ΔN) was calculated and its value is given in Table 6. If $\Delta N < 3.6$ (electron), the inhibition efficiency increases with increasing value of ΔN , while it decreased if $\Delta N > 3.6$ (electron)

[68,69]. In present contribution, Pyr2 is the donor of electrons, and the iron surface atom was the acceptor. The Pyr2 was bound to the mild steel surface, and thus formed inhibition adsorption layer against corrosion at mild steel/hydrochloric acid solution interface.

CONCLUSION

Ethyl 6-amino-5-cyano-2-methyl-4-(p-tolyl)-4H-pyran-3-carboxylate (Pyr2) is a good inhibitor for corrosion of mild steel in 1.0 M HCl, and the inhibition efficiency increases with increase in the concentration of the Pyr2 but decreases with rise in temperature. Polarization measurements show that Pyr2 inhibits both the anodic and cathodic processes of the corrosion of mild steel in 1.0 M HCl solution, which is a mixed type corrosion inhibitor. EIS results showed that as the inhibitor concentration increased the charge transfer resistance increased and the double layer capacity decreased. Pyr2 acted through adsorption on the mild steel surface and its adsorption obeyed the Langmuir adsorption isotherm. The value of free Gibbs energy showed that compound was adsorbed on the steel surface via chemical adsorption. Theoretical calculations provide good support to experimental results.

REFERENCES

- [1] H. Ashassi-Sorkhabi, D. Seifzadeh, M.G. EN. Hosseini, *Corros. Sci.* **2008**, 50, 3363.
- [2] M.A. Ameer, E. Khamis, G. Al-Senani, *Adsorpt. Sci. Technol.* **2000**, 18, 177.
- [3] M.S. Morad, A.M. Kamal El-Dean, *Corros. Sci.* **2006**, 48, 3398.
- [4] A. Popova, E. Sokolova, S. Raicheva, M. Christov, *Corros. Sci.* **2003**, 45, 33.
- [5] S. Karthikeyan, H.K. Sappani, G. Venkatachalam, S. Narayanan, *Int. J. Chem. Tech Res.* **2012**, 4, 910.
- [6] A.K. Singh, *Ind. Eng. Chem. Res.* **2012**, 51, 3215.
- [7] M.A. Chidiebere, C.E. Oguke, K.L. Oguzie, C.N. Eneh, E.E. Oguzie, *Ind. Eng. Chem. Res.* **2012**, 51, 668.
- [8] A.H. Al Hamzi, H. Zarrok, A. Zarrouk, R. Salghi, B. Hammouti, S.S. Al-Deyab, M. Bouachrine, A. Amine, F. Guenoun, *Int. J. Electrochem. Sci.*, **2013**, 8, 2586.
- [9] A. Zarrouk, B. Hammouti, H. Zarrok, I. Warad, M. Bouachrine, *Der Pharm. Chem.*, **2011**, 3, 263.
- [10] D. Ben Hmamou, R. Salghi, A. Zarrouk, M. Messali, H. Zarrok, M. Errami, B. Hammouti, Lh. Bazzi, A. Chakir, *Der Pharm. Chem.*, **2012**, 4, 1496.
- [11] A. Ghazoui, N. Bencat, S.S. Al-Deyab, A. Zarrouk, B. Hammouti, M. Ramdani, M. Guenbour, *Int. J. Electrochem. Sci.*, **2013**, 8, 2272.
- [12] A. Zarrouk, H. Zarrok, R. Salghi, N. Bouroumane, B. Hammouti, S.S. Al-Deyab, R. Touzani, *Int. J. Electrochem. Sci.*, **2012**, 7, 10215.
- [13] H. Bendaha, A. Zarrouk, A. Aouniti, B. Hammouti, S. El Kadiri, R. Salghi, R. Touzani, *Phys. Chem. News*, **2012**, 64, 95.
- [14] S. Rekkab, H. Zarrok, R. Salghi, A. Zarrouk, Lh. Bazzi, B. Hammouti, Z. Kabouche, R. Touzani, M. Zougagh, *J. Mater. Environ. Sci.*, **2012**, 3, 613.
- [15] A. Zarrouk, B. Hammouti, H. Zarrok, M. Bouachrine, K.F. Khaled, S.S. Al-Deyab, *Int. J. Electrochem. Sci.*, **2012**, 6, 89.
- [16] A. Ghazoui, R. Saddik, N. Benchat, M. Guenbour, B. Hammouti, S.S. Al-Deyab, A. Zarrouk, *Int. J. Electrochem. Sci.*, **2012**, 7, 7080.
- [17] H. Zarrok, K. Al Mamari, A. Zarrouk, R. Salghi, B. Hammouti, S. S. Al-Deyab, E. M. Essassi, F. Bentiss, H. Oudda, *Int. J. Electrochem. Sci.*, **2012**, 7, 10338.
- [18] S.A. Ali, M.T. Saeed, S.V. Rahman, *Corros. Sci.* **2003**, 45, 253.
- [19] D.K. Yadav, M.A. Quraishi, *Ind. Eng. Chem. Res.* **2012**, 51, 8194.
- [20] M. Gopiraman, N. Selvakumaran, D. Kesavan, I.S. Kim, R. Karvembu, *Ind. Eng. Chem. Res.* **2012**, 51, 7910.
- [21] S. Karthikeyan, S. Hari Kumar, G. Venkatachalam, S. Narayanan, R. Venckatesh, *Int. J. Chem. Tech. Res.* **2012**, 4, 1065.
- [22] J.-J. Fu, H.-S. Zang, Y. Wang, S.-N. Li, T. Chen, X.-D. Liu, *Ind. Eng. Chem. Res.* **2012**, 51, 6377.
- [23] H. Zarrok, A. Zarrouk, R. Salghi, Y. Ramli, B. Hammouti, M. Assouag, E. M. Essassi, H. Oudda and M. Taleb, *J. Chem. Pharm. Res.*, **2012**, 4, 5048.
- [24] A. Zarrouk, B. Hammouti, A. Dafali, F. Bentiss, *Ind. Eng. Chem. Res.* **2013**, 52, 2560.
- [25] H. Zarrok, A. Zarrouk, R. Salghi, H. Oudda, B. Hammouti, M. Assouag, M. Taleb, M. Ebn Touhami, M. Bouachrine, S. Boukhris, *J. Chem. Pharm. Res.* **2012**, 4, 5056.
- [26] H. Zarrok, H. Oudda, A. El Midaoui, A. Zarrouk, B. Hammouti, M. Ebn Touhami, A. Attayibat, S. Radi, R. Touzani, *Res. Chem. Intermed.* **2012**, 38, 2051.
- [27] A. Ghazoui, A. Zarrouk, N. Bencat, R. Salghi, M. Assouag, M. El Hezzat, A. Guenbour, B. Hammouti, *J. Chem. Pharm. Res.* **2014**, 6, 704.
- [28] H. Zarrok, A. Zarrouk, R. Salghi, M. Ebn Touhami, H. Oudda, B. Hammouti, R. Tourir, F. Bentiss, S.S. Al-Deyab, *Int. J. Electrochem. Sci.* **2013**, 8, 6014.

- [29] A. Zarrouk, H. Zarrok, R. Salghi, R. Touir, B. Hammouti, N. Benchat, L.L. Afrine, H. Hannache, M. El Hezzat, M. Bouachrine, *J. Chem. Pharm. Res.* **2013**, 5, 1482.
- [30] H. Zarrok, A. Zarrouk, R. Salghi, M. Assouag, B. Hammouti, H. Oudda, S. Boukhris, S.S. Al Deyab, I. Warad, *Der Pharm. Lett.* **2013**, 5, 43.
- [31] D. Ben Hmamou, M.R. Aouad, R. Salghi, A. Zarrouk, M. Assouag, O. Benali, M. Messali, H. Zarrok, B. Hammouti, *J. Chem. Pharm. Res.* **2012**, 4, 3498.
- [32] M. Belayachi, H. Serrar, H. Zarrok, A. El Assyry, A. Zarrouk, H. Oudda, S. Boukhris, B. Hammouti, Eno E. Ebenso, A. Geunbour, *Int. J. Electrochem. Sci.* **2015**, 10, 3010.
- [33] H. Tayebi, H. Bourazmi, B. Himmi, A. El Assyry, Y. Ramli, A. Zarrouk, A. Geunbour, B. Hammouti, Eno E. Ebenso, *Der Pharm. Lett.* **2014**, 6(6), 20.
- [34] H. Tayebi, H. Bourazmi, B. Himmi, A. El Assyry, Y. Ramli, A. Zarrouk, A. Geunbour, B. Hammouti, *Der Pharm. Chem.* **2014**, 6(5), 220.
- [35] A. D. Becke, *J. Chem. Phys.* **1992**, 96, 9489.
- [36] A. D. Becke, *J. Chem. Phys.* **1993**, 98, 1372.
- [37] C. Lee, W. Yang, R.G. Parr, *Phys. Rev. B* **1988**, 37, 785.
- [38] M.J. Frisch, G.W. Trucks, H.B. Schlegel, G.E. Scuseria, M.A. Robb, J.R. Cheeseman, J.A. Montgomery Jr., T. Vreven, K.N. Kudin, J.C. Burant, J.M. Millam, S.S. Iyengar, J. Tomasi, V. Barone, B. Mennucci, M. Cossi, G. Scalmani, N. Rega, G.A. Petersson, H. Nakatsuji, M. Hada, M. Ehara, K. Toyota, R. Fukuda, J. Hasegawa, M. Ishida, T. Nakajima, Y. Honda, O. Kitao, H. Nakai, M. Klene, X. Li, J.E. Knox, H.P. Hratchian, J.B. Cross, C. Adamo, J. Jaramillo, R. Gomperts, R.E. Stratmann, O. Yazyev, A.J. Austin, R. Cammi, C. 870 H. Ju et al. / *Corrosion Science* 50 (2008) 865-871 Pomelli, J.W. Ochterski, P.Y. Ayala, K. Morokuma, G.A. Voth, P. Salvador, J.J. Dannenberg, V.G. Zakrzewski, S. Dapprich, A.D. Daniels, M.C. Strain, O. Farkas, D.K. Malick, A.D. Rabuck, K. Raghavachari, J.B. Foresman, J.V. Ortiz, Q. Cui, A.G. Baboul, S. Clifford, J. Cioslowski, B.B. Stefanov, G. Liu, A. Liashenko, P. Piskorz, I. Komaromi, R.L. Martin, D.J. Fox, T. Keith, M.A. Al-Laham, C.Y. Peng, A. Nanayakkara, M. Challacombe, P.M.W. Gill, B. Johnson, W. Chen, M.W. Wong, C. Gonzalez, J.A. Pople, Gaussian 03, Revision C.02, Gaussian Inc., Pittsburgh, PA, **2003**.
- [39] C.B. Verma, M.J. Reddy, M.A. Quraishi, *Anal. Bioanal. Electrochem.* **2014**, 6, 321.
- [40] M.A. Veloz, I. González, *Electrochim. Acta* **2002**, 48, 135.
- [41] M. Faustin, A. Maciuk, P. Salvin, C. Roos, M. Lebrini, *Corros. Sci.* **2015**, 92, 287.
- [42] C.B. Verma, P. Singh, I. Bahadur, E.E. Ebenso, M.A. Quraishi, *J. Mol. Liq.* **2015**, 209, 767.
- [43] X. Zhou, H. Yang, F. Wang, *Electrochim. Acta* **2011**, 56, 4268.
- [44] M. Valcarce, M. Vázquez, *Electrochim. Acta* **2008**, 53, 5007.
- [45] A. Yousefi, S. Javadian, N. Dalir, J. Kakemam, J. Akbari, *RSC Adv.* **2015**, 5, 11697.
- [46] A.S. El-Tabei, M.A. Hegazy, *J. Surfactant Deterg.* **2013**, 16, 757.
- [47] E.S. Ferreira, C. Giancomelli, F.C. Giacomelli, A. Spinelli, *Mater. Chem. Phys.* **2004**, 83, 129.
- [48] O.L. Riggs, Jr. *Corrosion Inhibitors*, 2nd ed.; C. C. Nathan: Houston, TX, USA, **1973**; p 109.
- [49] M.A. Quraishi, A. Singh, V. Singh, D. Yadav, A.K. Singh, *Mater. Chem. Phys.* **2010**, 122, 114.
- [50] R. Solmaz, G. Kardas, M.C. Ulha, B. Yazıcı, M. Erbil, *Electrochim. Acta* **2008**, 53, 5941.
- [51] W. Chen, H.Q. Luo, N.B. Li, *Corros. Sci.* **2011**, 53, 3356.
- [52] S.S. Abd El-Rehim, M.A.M. Ibrahim, K.F. Khaled, *J. Appl. Electrochem.* **1999**, 29, 593.
- [53] S. Martinez, I. Stern, *Appl. Surf. Sci.* **2002**, 199, 83.
- [54] M. Dahmani, A. Et-Touhami, S.S. Al-Deyab, B. Hammouti, A. Bouyanzer, *Int. J. Electrochem. Sci.* **2010**, 5, 1060.
- [55] G. Avci, *Mater. Chem. Phys.* **2008**, 112, 234.
- [56] E. Bayol, A.A. Gurten, M. Dursun, K. Kayakırılmaz, *Acta Phys. Chim. Sin.* **2008**, 24, 2236.
- [57] O.K. Abiola, N.C. Oforka, *Mater. Chem. Phys.* **2004**, 83, 315.
- [58] M. Ozcan, R. Solmaz, G. Kardas, I. Dehri, *Colloid Surf. A.* **2008**, 325, 57.
- [59] F. Hongbo, "Synthesis and application of new type inhibitors", Chemical Industry Press, Beijing, **2002**, p.166.
- [60] I.B. Obot, N.O. Obi-Egbedi, *Corros. Sci.* **2010**, 52, 657.
- [61] Fu Jiajun, Haishan Zang, Ying Wang, Suning Li, Tao Chen, Xiaodong Liu, *Ind. Eng. Chem. Res.* **2012**, 51, 6377.
- [62] Jiajun Fu, Suning Li, Ying Wang, Xiaodong Liu, Lude Lu, *J. Mater. Sci.* **2011**, 46, 3550.
- [63] N.O. Obi-Egbedi, I.B. Obot, *Corros. Sci.* **2011**, 53, 263.
- [64] M. Behpour, S.M. Ghoreishi, M. Khayat Kashani, N. Soltani, *Corros. Sci.* **2011**, 53, 2489.
- [65] Dileep Kumar Yadav, M.A. Quraishi, B. Maiti, *Corros. Sci.* **2012**, 55, 254.
- [66] V.S. Sastri, J.R. Perumareddi, *Corrosion*, **1997**, 53, 617.
- [67] F. Bentiss, M. Traisnel, M. Lagrenee, *Corros. Sci.*, **2000**, 42, 127.
- [68] F. Bentiss, M. Traisnel, *J. Appl. Electrochem.*, **2001**, 31, 41.
- [69] I. Lukovits, E. Kalman, F. Zucchi, *Corrosion*, **2001**, 57, 3.